A Design Method for Cage Induction Motors with Non-Skewed Rotor Bars

Zhao Haisen, Wang Xiangyu, Wang Qing, Liu Xiaofang, and Luo Yingli
School of Electric and Electronics Engineering, North China Electric Power University
No. 2 Beinong Road, Huilongguan, Changping District, Beijing, 102206, China
zhaohisen@163.com

***Abstract*—This paper presents a design method for non-skewed small and medium cage induction motor based on the finite element analysis, in which the approaches of asymmetrical rotor slots, closed slots, reasonable slot combination and air-gap length are adopted and studied systematically. With this method, the cage induction motors with non-skewed rotor bars can be realized meanwhile, the slot harmonic, which is caused by slot opening, can be eliminated effectively and the total losses can also be decreased apparently. Finally, the experimental validation of a 5.5 kW induction motor is performed.**

***Index Terms*— Cage induction motor, losses, non-skewed rotor, time-stepping finite element method (T-S FEM).**

I. INTRODUCTION

Generally, skewed rotors are used to weaken the additional torque and noise caused by slot harmonics field in the traditional design of small and medium cage induction motors. In such cases, The skewed rotor can reduce harmonic copper loss caused by stator and rotor harmonic currents; however there is also a corresponding increase in the non-uniform field distribution along the axial direction, which leads to greater core saturation and higher iron losses [1-2]. Furthermore, the skewed rotor may cause the excess loss due to the transverse current between rotor bars, which has a great proportion in total excess losses of the small and medium motors, while the starting torque may be decreased [3-4]. Therefore, to improve the efficiency and operating performance of the induction motors, it is necessary to study how to avoid the skewed rotor in cage induction motors.

This paper intends to develop a new design method for avoiding the skewed rotors, by which the excess losses of the induction motors can be reduced effectively and the starting performance can also be maintained and improved.

II. FINITE ELEMENT ANALYSIS AND DESIGN METHOD DESCRIPTION

A. Multi-Slice Field-Circuit T-S FEM

Due to the skewed rotor bars, the EMF induced by slot harmonic in rotor bar can be eliminated along with axial direction. Theoretically, slot harmonic can also be weakened by adjusting the spatial positions of the rotor bars reasonably, and the key point is how to select the asymmetric distribution degree correctly. However, the analytical method is difficult to analyze the problem which is the magnetic field reaction caused by asymmetrical rotor bars. Therefore, the multi-slice field-circuit coupling T-S FEM is used and the coupled field and stator and rotor circuit equations are given as follows.

$$\begin{bmatrix} \boldsymbol{K}_{\mathrm{A}(1,\theta)} & 0 & 0 & 0 & \boldsymbol{K}_{\mathrm{s}(1,\theta)} & \boldsymbol{K}_{\mathrm{r}(1,\theta)} \\ 0 & \boldsymbol{K}_{\mathrm{A}(2,\theta)} & 0 & 0 & \boldsymbol{K}_{\mathrm{s}(2,\theta)} & \boldsymbol{K}_{\mathrm{r}(2,\theta)} \\ 0 & 0 & \cdots & 0 & \cdots & \cdots \\ 0 & 0 & 0 & \boldsymbol{K}_{\mathrm{A}(k,\theta)} & \boldsymbol{K}_{\mathrm{s}(k,\theta)} & \boldsymbol{K}_{\mathrm{r}(k,\theta)} \\ 0 & 0 & 0 & 0 & \boldsymbol{R}_{\mathrm{s}} & 0 \\ 0 & 0 & 0 & 0 & 0 & \boldsymbol{R}_{\mathrm{r}} \end{bmatrix} \begin{bmatrix} \boldsymbol{A}_{(1)} \\ \boldsymbol{A}_{(2)} \\ \cdots \\ \boldsymbol{A}_{(k)} \\ \boldsymbol{I}_{\mathrm{s}} \\ \boldsymbol{I}_{\mathrm{r}} \end{bmatrix} + \begin{bmatrix} \boldsymbol{D}_{\mathrm{A}(1,\theta)} & 0 & 0 & 0 & 0 & 0 \\ 0 & \boldsymbol{D}_{\mathrm{A}(2,\theta)} & 0 & 0 & 0 & 0 \\ 0 & 0 & \cdots & 0 & 0 & 0 \\ 0 & 0 & 0 & \boldsymbol{D}_{\mathrm{A}(k,\theta)} & 0 & 0 \\ \boldsymbol{D}_{\mathrm{s}(1,\theta)} & \boldsymbol{D}_{\mathrm{s}(2,\theta)} & \cdots & \boldsymbol{D}_{\mathrm{s}(k,\theta)} & \boldsymbol{R}_{\mathrm{s}} & 0 \\ \boldsymbol{D}_{\mathrm{r}(1,\theta)} & \boldsymbol{D}_{\mathrm{r}(2,\theta)} & \cdots & \boldsymbol{D}_{\mathrm{r}(k,\theta)} & 0 & \boldsymbol{R}_{\mathrm{r}} \end{bmatrix} \begin{bmatrix} \boldsymbol{A}_{(1)} \\ \boldsymbol{A}_{(2)} \\ \cdots \\ \boldsymbol{A}_{(k)} \\ \boldsymbol{I}_{\mathrm{s}} \\ \boldsymbol{I}_{\mathrm{r}} \end{bmatrix}' = \begin{bmatrix} 0 \\ 0 \\ 0 \\ 0 \\ \boldsymbol{U}_{\mathrm{S}} \\ 0 \end{bmatrix} \tag{1}$$

In (1), $\boldsymbol{K}_{\mathrm{A}(n,\theta)}$ is the stiffness matrix of field equations. $\boldsymbol{K}_{\mathrm{s}(n,\theta)}$ and $\boldsymbol{K}_{\mathrm{r}(n,\theta)}$ are the coupled matrix between the nodal vector magnetic potential and the relevant current terms in stator and rotor circuit. $\boldsymbol{D}_{\mathrm{A}(n,\theta)}$, $\boldsymbol{D}_{\mathrm{s}(n,\theta)}$ and $\boldsymbol{D}_{\mathrm{s}(n,\theta)}$ are the matrix that corresponds to the derivative terms of nodal vector magnetic potential in the field equation and stator and rotor circuit equations, respectively. $\boldsymbol{A}_{(\mathrm{n})}$ is the nodal magnetic potential vector. Among the above variables, "n" is the corresponding matrix (n=1,2,…,k) of the n^{th} straight rotor, and each matrix is a function of skew angle θ. $\boldsymbol{I}_{\mathrm{s}}$ and $\boldsymbol{I}_{\mathrm{r}}$ are the vector of stator currents and rotor end ring currents, respectively. "′" is the symbol of derivation, standing for the derivation of each state variable with respect to time. $\boldsymbol{U}_{\mathrm{s}}$ is the matrix of supply voltages. Then, the backwards difference Euler method is used to solve the equation after the spatial and time discretiztion.

B. Design Method Description

The design method for non-skewed small and medium cage induction motors are presented as follows.

1) Considering that the axially symmetrical structure can be accomplished easily by the sine wave modulation, so the asymmetrical rotor slots with the sine wave modulation are adopted, and the spatial positions of each slot can be determined by following formula.

$$\theta_n = \theta_{n0} + K\zeta \tag{2}$$

Where, θ_{n} is the spatial position of the n^{th} rotor slot, θ_{n0} is the spatial position with even rotor slots distribution, which can be obtained by equation $\theta_{\mathrm{n0}}=2\pi n/Z_2$, Z_2 is the rotor slot number. K is the modulate coefficient of spatial position, its value is in the range of 0~0.03; ζ is the angle obtained by the sine modulated method, it can be described as $\zeta=\sin(2\pi n\varepsilon/Z_2)$, ε is the coefficient of the sine wave, it can be set as 0~4.

2) Besides the asymmetrical rotor slots, closed slots are used to further eliminate the influence of the slot harmonic on the motor losses and noise. Considering the demand of the

mechanical strength, the height of the closed slot bridge is set as 0.5mm~3mm for the motors with different capacities.

3) Based on two measures taken above, the slot harmonic can be eliminated to a great extent. Therefore, the slot combination can be selected in a wide range, namely, the slot numbers in rotor side should be close to the ones in stator side, which should be according to the equation $Z_2>0.9Z_1$.

4) With the closed slot, slot leakage flux is increased so that the starting performance is weakened. To solve this problem, the air-gap length can be adjusted reasonably as the harmonic field is reduced by the first and second measures, by which the starting performance is maintained and improved, that is, it should be reduced 0.02mm~1mm for the different motor sizes.

III. A Design Example of 5.5 kW Cage Induction Motor

A. Determination on the Parameters of the Improved Rotor

With the asymmetric rotor slots, the magnetic circuit inside the motor may be asymmetric, which leads to the fluctuating reluctance and then affects the operating performance of the motors. Therefore, after the selection of the primary parameter as the methods in section II, the minor modification should be performed with the multi-slice field-circuit coupling T-S FEM, in which the skill of adaptive re-meshing is adopted to reduce the time consuming.

Due to the contents limit, the details of the modulate coefficient of spatial position, coefficient of the sine wave, height of the closed rotor bridge, slot combination and air-gap length determination, will be given in full paper.

B. Improved Rotor Structure of 5.5 kW Motor

The improved rotor structure is given in Fig. 1. And the detailed parameters are as follows: the modulate coefficients K and ζ are set as 0.02 and 4 respectively, by which the fluctuating reluctance is not apparent. The slot combination is changed from 36/32 to 36/33, and the height of the closed slot bridge and the air-gap length are set as 1mm and 0.35mm, respectively. Further, the flux density distribution is given in Fig.2, it can be seen that the flux density distribution of the improved rotor is similar to the initial one.

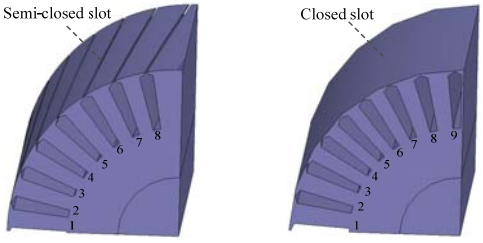

(a) Initial (b) Improved

Fig.1 Comparison of the initial and improved rotor structure

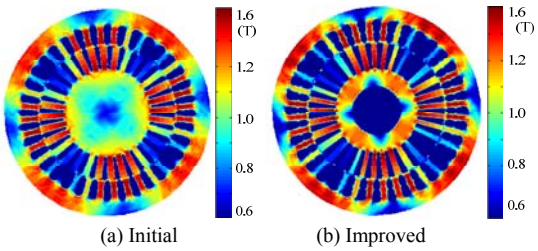

(a) Initial (b) Improved

Fig.2 Comparison of flux density distribution of initial and improved motor

IV. Experimental Validation

The improved rotor and 5.5 kW prototype motor are given in Fig.3 and the tested phase-A stator currents and harmonic spectrum are given in Fig.4 and Fig.5. It can be seen that, comparing with the skewed motor, the slot harmonic component of stator current is eliminated effectively. Further, the different load test is also performed as the method B in IEEE Std. 112-2004. It is shown that the total losses with no-load condition decrease by 6.7%, from 310 W to 289 W. And the comparison of motor losses with half- and full-load conditions are given in Table 1, in which P_1 and P_2 are input and output active power, Q and PF are reactive power and power factor, P_{cu1} and P_{cu2} are stator and rotor copper losses, P_{fe} and P_s are iron loss and stray loss, P_Σ is total losses. It is noted that the friction loss is 50 W, which is not given in the table as it can be assumed as a constant value during the test.

(a) The improved non-skewed rotor (b) The prototype

Fig.3 Improved non-skewed rotor and the prototype

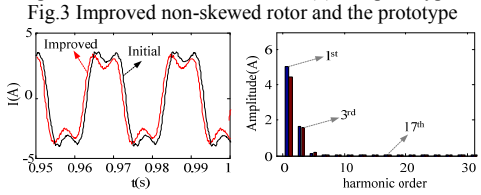

Fig.4 Comparison of phase-A stator current and harmonic spectrum analysis with no-load condition

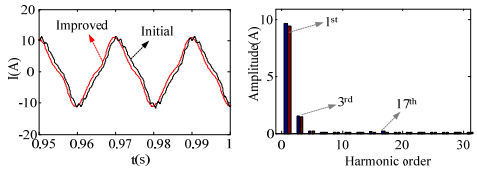

Fig.5 Comparison of phase-A stator current and harmonic spectrum analysis with full-load condition

Table 1 Comparison of motor loss with half- and full- load conditions

	Load	P_1	P_2	Q	PF	P_{cu1}	P_{cu2}	P_{fe}	P_s	P_Σ
Initial	50%P_N	3230	2810	4395	0.59	163	41	153	12	420
	P_N	6279	5520	4820	0.79	343	166	150	50	759
Improved	50%P_N	3229	2812	4146	0.61	151	41	157	18	417
	P_N	6346	5561	4462	0.82	330	176	153	75	785

References

[1] Catherine I. McClay, Stephen Williamson, "The variation of cage motor losses with skew," *IEEE Trans Ind Appl.*, vol.36, no. 6, 1563-1570, Nov./Dec., 2000.

[2] Zhao Haisen, Liu Xiaofang, Luo Yingli, Chen Weihua, and Peter Baldassari, "Time-stepping finite element analysis on the influence of skewed rotors and different skew angles on the losses of squirrel cage asynchronous motors," *Sci China Tech Sci*, vol. 54, no. 9, pp. 2511-2519, Sep. 2011.

[3] David G. Dorrel, Piotr J. Holik, and Claus B. Rasmussen, "Analysis and effects of inter-bar current and skew on a long skewed-rotor induction motor for pump applications," *IEEE Trans Magn.*, vol. 43, no. 6, pp. 2534-2536, June 2007

[4] David G. Dorrel, Piotr J. Holik, Patrick Lombard, and Hans Jorgen Thougaard, "A Multisliced finite-element model for induction machines incorporating interbar current," *IEEE Trans Ind Appl.*, vol. 45, no. 1, pp. 131-141, Jan./Feb., 2009.